Journal of Geographic Information System, 2025, 17(5), 291-323
https://www.scirp.org/journal/jgis
ISSN Online: 2151-1969
ISSN Print: 2151-1950

Remote Sensing Assessment of Multi-Decadal Land-Use Change and ESV Decline in Peri-Urban Highland Corridors: The Case of the Santa-Babadjou Corridor in Cameroon

Besende Didien Njumba[1*], Mary Lum Fonteh Niba[2], Banseka JaneFrances Yenlajai[1]

[1]Department of Geography and Planning, The University of Bamenda, Bamenda, Cameroon
[2]Department of Geography, Higher Teachers Training College, The University of Bamenda, Bamenda, Cameroon
Email: *besnju@gmail.com, mariefontehniba3@gmail.com, jbanseka@yahoo.com

How to cite this paper: Njumba, B.D., Niba, M.L.F. and Yenlajai, B.J.F. (2025) Remote Sensing Assessment of Multi-Decadal Land-Use Change and ESV Decline in Peri-Urban Highland Corridors: The Case of the Santa-Babadjou Corridor in Cameroon. *Journal of Geographic Information System*, **17**, 291-323.
https://doi.org/10.4236/jgis.2025.175014

Received: August 24, 2025
Accepted: September 25, 2025
Published: September 28, 2025

Abstract

Rapid peri-urbanization in agricultural highland corridors can erode natural capital and undermine water security, yet few studies provide spatially explicit, multi-decadal valuations of ecosystem services for such rurbanizing landscapes. Here, we quantified land-use/land-cover (LULC) dynamics and ecosystem service valuation (ESV) for the Santa-Babadjou corridor from 1980-2024 using multi-temporal Landsat imagery, rigorous preprocessing (radiometric correction), k-means classification into five LULC classes, and benefit-transfer valuation based on Costanza's coefficients to estimate total ESV and 17 ecosystem functions. Results reveal significant landscape and value losses, with built-up expanding from 4,430 ha (6.1%) to 32,709.5 ha (44.9%) in 2024, while forest cover fell from 26,783 ha (36.7%) to 6,620.7 ha (9.1%) (−75.3%) and grasslands from 27,929.6 ha (38.3%) to 11,848.3 ha (16.2%) (−57.6%). Correspondingly, total ESV collapsed from US$220.12 million in 1980 to US$33.70 million in 2024 (−84.7%), with the steepest losses occurring in the period after 2010, in which forests and grasslands, which contributed ≈99% of ESV in 1980, dropped to US$2.20 M and US$9.97 M respectively by 2024. Functionally, provisioning, regulating, supporting, and cultural service totals all declined markedly, with provisioning services falling from US$108.2M to US$58.8 M; regulating from US$90.2 M to US$48.4 M. Cumulatively, these changes signal widespread degradation in hydrological regulation, soil retention, and biodiversity support. These spatially explicit, quantitative findings highlight that unplanned settlement and agricultural intensification are compromising the corridor's natural capital and water-security functions. We therefore recommend immediate policy action to protect the remaining forest and recharge zones, restore de-

graded catchments using nature-based solutions, and integrate ESV metrics into land-use planning and participatory decision-making to arrest value loss and rebuild resilience.

Keywords

Ecosystem Service Valuation (ESV), Highland Corridors, Land-Use/Land-Cover Change (LULC), Natural Capital, Peri-Urbanization, Remote Sensing, Water Security

1. Introduction

Ecosystem services (ES) are the essential ecological processes and conditions through which natural ecosystems and the diverse species within them support, sustain, and enrich human life [1]-[3]. In communities where agriculture remains the dominant land use, yet where rapid population growth and peri-urban expansion are reshaping landscapes, ES serve as a vital bridge between natural systems and socio-economic development [1]. These services encompass the direct and indirect benefits derived from ecosystem functions and are generally classified into four categories: (a) provisioning services: food, freshwater, fuelwood, and medicinal resources; (b) regulating services: water purification, erosion control, flood regulation, and microclimate moderation; (c) supporting services: soil formation, nutrient cycling, and pollination that underpin agricultural productivity; and (d) cultural services: recreational, spiritual, and cultural value rooted in local landscapes and traditions [1]. In rurbanizing agricultural communities, where traditional rural livelihoods increasingly intersect with urban pressures, the functionality of ecosystems becomes central to sustainability [4]. Ecosystem services not only sustain agriculture and food systems but also help mitigate the impacts of land use change, deforestation, habitat fragmentation, and declining water quality [4] [5]. As identified by [2] [6], at least 17 key ecosystem functions contribute to the health, stability, and resilience of human-environment systems, many of which are particularly crucial in these transitioning zones. The growing strain on land, water, and other natural resources in such areas amplifies the importance of healthy ecosystems in providing vital services like groundwater recharge, waste assimilation, biodiversity support, and temperature regulation. Preserving and enhancing these services is fundamental to ensuring the long-term viability of agriculture, safeguarding water security, and improving human well-being.

Yet, in these transitioning landscapes, the benefits of ES are increasingly at risk due to intensifying anthropogenic pressures. Sustained population growth, rural-to-urban migration, climate variability, expanding infrastructure, and shifting agricultural practices are collectively placing unprecedented strain on the natural systems that underpin local livelihoods. As demand rises for land, food, water, and

energy, the capacity of ecosystems to regenerate and provide essential services is steadily diminishing [7]-[10]. Over the past several decades, the pace and scale at which ecosystems have been altered to meet human needs, whether for settlement expansion, intensified cultivation, or resource extraction, have led to widespread degradation. This loss of ecosystem functionality directly undermines efforts to improve health, reduce poverty, and achieve sustainable development at the community level [11]-[14]. In rurbanizing areas, such degradation can manifest in declining soil fertility, water contamination, biodiversity loss, increased erosion, and heightened vulnerability to climate-related hazards such as floods and droughts.

Among the most influential drivers of change in these regions is the transformation of land use and land cover (LULC), particularly the conversion of forest, grassland, wetlands, and agricultural land into built-up or degraded spaces [15]-[18]. These shifts are not only more rapid and intense than in previous decades, but they also exhibit complex spatial and temporal patterns. For example, replacing floodplains or forest buffers with impervious surfaces can significantly disrupt local hydrological cycles, leading to reduced groundwater recharge, increased surface runoff, and higher flood risks during rainfall events [1] [5] [8] [19]. The impacts of LULC change on ES are dynamic and context-specific, varying across topographies, ecological zones, and socio-economic settings [7] [20]-[22]. As such, monitoring ecosystem health and understanding its interactions with community well-being have become crucial areas of research and policy interest. Effective planning in these rurbanizing agricultural corridors must go beyond sectoral approaches and embrace integrated frameworks that account for environmental sustainability, economic needs, and social equity. Recognizing the central role of ecosystem services in these landscapes is therefore indispensable for building resilient communities and fostering long-term development [23] [24].

A wide range of methodological approaches has been developed to evaluate terrestrial ES, each varying in complexity, data requirements, and application context. These valuation methods are generally grouped into four broad categories: (a) revealed preference approaches, which infer value based on actual market behavior; (b) stated preference approaches, which rely on survey-based techniques to capture hypothetical willingness to pay; (c) cost-based approaches, which estimate value through the cost of replacing or restoring ecosystem functions; and (d) the benefit transfer method (BTM), which involves applying valuation estimates from existing studies to new contexts [25]-[31].

Among these, the benefit transfer method has gained widespread popularity due to its efficiency, scalability, and ease of application, especially in data-scarce regions. First introduced by [32] in 1997, this approach involved classifying global ecosystems into 16 biomes and identifying 17 key ecosystem functions. Using secondary data from prior valuation studies, they estimated the global annual value of ecosystem services to be approximately USD 33 trillion (1995 values). This pioneering work significantly elevated the prominence of ecosystem service valuation within environmental research and policy discourse.

Since then, the BTM has been applied across various geographic and ecological contexts to assess the impacts of LULC change on ESV. For instance, [27] [33] investigated how shifts in LULC influenced ecosystem services in Chengdu, China; [9] explored the relationship between spatial scale and stakeholder valuation of ecosystem services; and [29] monitored the effects of LULC changes on ecosystem functions in Ethiopia's central highlands. Similarly, [16] examined the consequences of converting agricultural and forest land into built-up areas in India, and reported a significant decline in ESV as a result of such transformations.

The Santa-Babadjou Corridor is a predominantly agro-economy-based region in the Western highlands of Cameroon, marked by increasing population density, ecological sensitivity, and growing exposure to climate variability and disaster risks. In recent years, the corridor has undergone notable socio-economic changes, such as infrastructure development, expansion of road networks, and the growth of local trade, which have contributed to a steady shift in land use patterns. As one of the key agricultural transition zones in the region, the corridor is witnessing accelerated rural-urban migration and uncoordinated spatial expansion, leading to major changes in LULC.

Recent research highlights that this peri-urban corridor is experiencing significant ecological stress due to rapid and often unplanned LULC transformations. Drivers such as population pressure, climate variability, economic activity, and infrastructural development have contributed to the decline of vegetation cover, conversion of farmlands into settlements, and the encroachment into wetlands and riparian zones [34]. These dynamics threaten the natural functioning of the local ecosystem and have resulted in land degradation, increased surface runoff, localized flooding, erosion, and a marked rise in the frequency of waterborne diseases [35]. For instance, built-up areas have expanded at the expense of farmland and ecologically sensitive zones, disrupting hydrological cycles and placing stress on existing drainage systems. As a result, soil fertility loss and water pollution have become recurrent issues affecting agricultural productivity and community health in the region.

In response to these challenges, we seek to explore the nexus between LULC change and ecosystem services in the Santa-Babadjou corridor. While comprehensive empirical work remains limited in this specific corridor, related studies in similar transitional zones in sub-Saharan Africa reveal parallel patterns. For example, studies have shown that agricultural land loss to built-up development results in significant declines in ESV, including losses in water regulation, soil retention, and food provision services. In some cases, these losses are valued at millions of dollars over a few decades due to unchecked land conversion [27] [36].

However, most of these existing studies focus either on urbanized cities or coastal zones, with limited attention given to highland transitional corridors such as the Santa-Babadjou corridors. Although some research efforts have applied satellite image-derived LULC analysis to assess ecosystem service dynamics, such methods are still underutilized in Cameroon's small-sized towns and peri-urban commu-

nities. Moreover, the relationship between LULC change and ESV in emerging corridors remains poorly understood, especially in regions where agriculture, population growth, and settlement development coexist in fragile ecological settings.

Given this gap, the current study aims to fill a critical research void by focusing on the Santa-Babadjou Corridor. Specifically, this study seeks to: (1) analyze the dynamics of LULC change in the corridor over 4 decades; (2) estimate and spatially map the total ESV during that time; (3) evaluate the contribution of individual ecosystem service functions to overall ESV; and (4) determine the elasticity of ESV in response to LULC changes. This approach will help clarify how ecological and human systems interact in transitional zones and offer evidence-based insights for sustainable land management and spatial planning.

2. Materials and Methods

2.1. Study Area

The Santa-Babadjou Corridor, spanning parts of the Northwest and West Regions of Cameroon, lies between latitudes 5˚42′ - 5˚54′ N and longitudes 10˚00′ - 10˚18′ E. The maps in **Figure 1** provide a visual representation of the corridor; Map 1a shows its position within the broader Northwest and West Regions; Map 1b highlights its placement within Mezam and Bamboutos Divisions; and Map 1c offers a detailed view of the corridor's geographic and agricultural features. The corridor connects the sub-divisional headquarters of Santa (in the Northwest) and Babadjou (in the West), functioning as a critical agricultural and transportation gateway between the two regions. The corridor is approximately 62 km from Bamenda, with Santa located 23 km and Babadjou 39 km away, and is bordered by Batibo, Lebialem, Menoua, Bali, Mbouda, Foumbot, Bamenda I & II, and Balikumbat subdivisions.

Covering about 1292 km^2, the corridor features a diverse landscape of mountains, valleys, forests, springs, cultivated fields, and clustered rural settlements. It is governed by a Guinea-type climate, with annual rainfall ranging from 2000 to 3000 mm and temperatures between 15˚C and 25˚C, shaping the region's agricultural patterns and water availability. Elevation across the corridor varies significantly, from 1300 meters in Bali-Gham and Awing to 2703 meters at the Wabane boundary. Notably, Mount Lefo in Awing (2300 m) is the second-highest peak in the Northwest Region.

Hydrologically, the region is drained by the Santa Stream and its dense network of tributaries, supporting irrigation and domestic water use. Soil types range from fertile alluvial soils in lowland floodplains (in Maforbe, Matazen, Kombou), to well-drained orthic soils in highland areas (in Akum, Baba, Mbu, Awing), and moisture-retentive humic soils in Santa. These diverse environmental characteristics enable intensive agriculture but also create varying pressures on the region's natural systems.

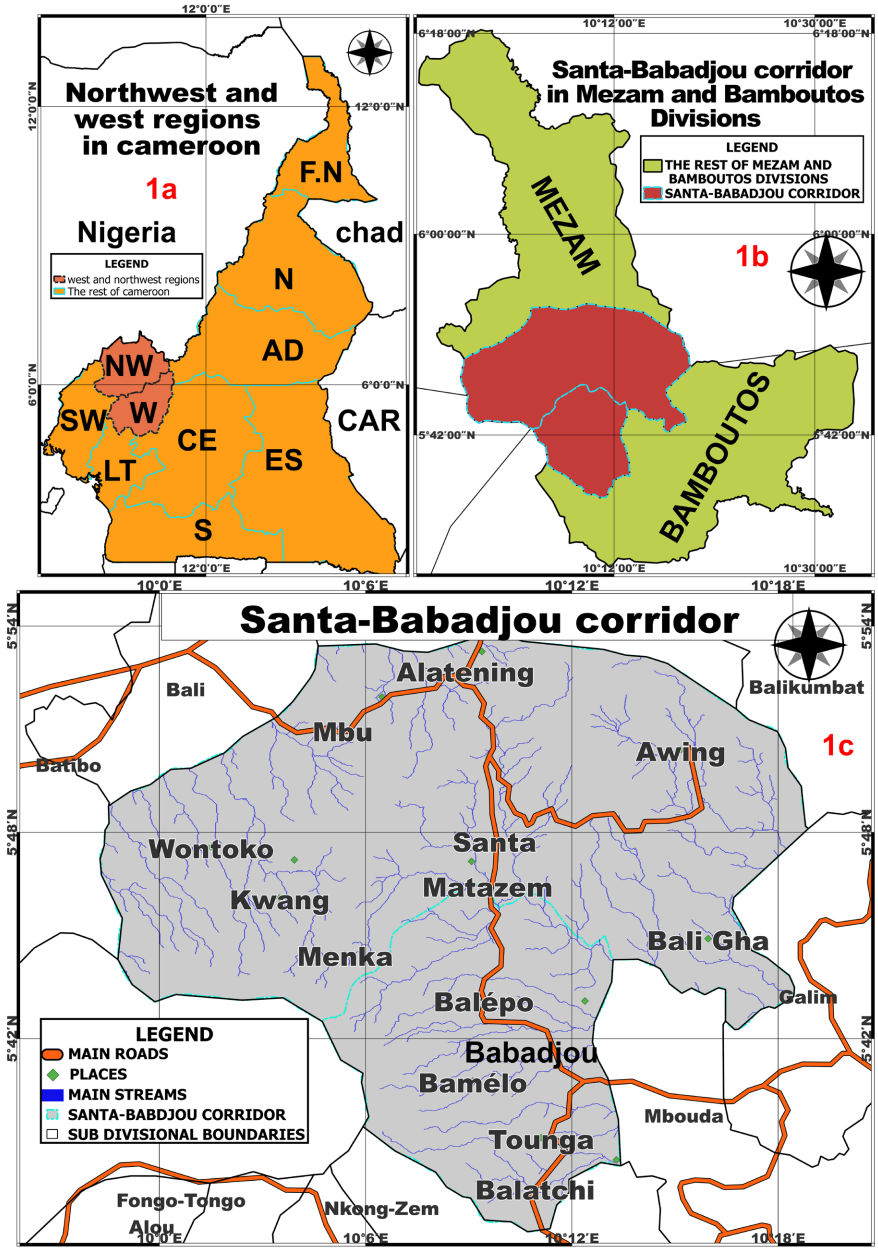

Figure 1. Location of the Santa-Babadjou corridor in the Mezam and Bamboutos divisions of Cameroon.

Recent trends in population growth, urban expansion, and agricultural intensification have led to rapid changes in land use and land cover (LULC) across the corridor. Natural vegetation and wetlands are increasingly being replaced by farms, roads, and built-up areas. This transformation has direct implications for the region's ESV (ESV), including declines in water regulation, soil retention, carbon sequestration, and biodiversity conservation.

As seen in similar contexts globally, such as in Dhaka, Bangladesh, unplanned LULC change without appropriate valuation of ecosystem services often leads to environmental degradation, resource scarcity, and diminished human well-being.

In the Santa-Babadjou Corridor, the lack of integrated planning and valuation threatens the sustainability of both agricultural productivity and water availability. Therefore, a robust assessment of ecosystem services is essential to inform land use decisions, ensure sustainable resource use, and maintain ecological integrity in this critical trans-regional corridor.

2.2. Datasets

This study focuses on the valuation of ecosystem services within the Santa-Babadjou Corridor, based on land use and land cover (LULC) change. LULC data form the primary basis for the analysis and were derived from multi-temporal satellite imagery. To capture the dynamics of change, a ten-year interval approach was applied, using Landsat datasets from Landsat-3, Landsat-5, Landsat-7, and Landsat-8. Landsat satellite images for the years 1980, 1990, 2000, 2010, 2020, and 2024 were acquired from the United States Geological Survey (USGS) archive (https://earthexplorer.usgs.gov/, accessed on 8 August 2025). This time frame allows for the assessment of long-term LULC transitions and their implications for ESVs (ESVs) in the corridor. Table 1 presents the detailed specifications of the Landsat images used for the analysis.

Table 1. Characteristics of Landsat images used in this study for the Santa-Babadjou Corridor.

Year	Satellite	Sensor	Path/Row	Resolution (m)
1980	Landsat 3	MSS	187/56	80
1990	Landsat 5	TM	187/56	30
2000	Landsat 7	ETM+	187/56	30
2010	Landsat 5	TM	187/56	30
2020	Landsat 8	OLI	187/56	30
2024	Landsat 9	OLI-2	187/56	30

MSS = Multispectral Scanner; TM = Thematic Mapper; *ETM+ = Enhanced Thematic Mapper Plus*; *OLI = Operational Land Imager*.

The entire Santa-Babadjou Corridor study area lies within Landsat path 187 and row 56. All satellite images used in this study were acquired with the Universal Transverse Mercator (UTM) projection in Zone 32 North, based on the World Geodetic System (WGS) 1984 datum. The spatial resolution of the selected images is 30 × 30 meters per pixel, ensuring sufficient detail for land use and land cover analysis.

To minimize the influence of seasonal variation on spectral reflectance, images were chosen to correspond to similar dates across different years. For this study, Landsat scenes from the month of November were prioritized, as this period falls in the dry season for the Santa-Babadjou Corridor. During November, cloud cover

is minimal, and the absence of significant rainfall reduces the risk of temporary inundation in low-lying areas being misclassified as wetlands or permanent water bodies. In cases where November images free of cloud cover were unavailable, such as in 1990, December imagery was used instead. This approach ensured consistent seasonal conditions across datasets, thereby improving the accuracy of land cover classification and water body detection within the corridor.

2.3. Landsat Image Processing

For this study, we downloaded Level-1 Precision and Terrain Corrected (L1TP) cloud-free multispectral images. These L1TP products are radiometrically calibrated and orthorectified using ground control points (GCPs) and a digital elevation model (DEM) to correct for relief displacement, an essential step given the corridor's complex topography, which ranges from low-lying valleys to mountain peaks above 2,700 meters [37]-[39]. The high geometric accuracy of L1TP data makes them suitable for pixel-level time series analysis without further geometric correction [40] [41].

The raw Landsat imagery contains digital number (DN) values for each pixel. These values do not directly represent the true characteristics of the Earth's surface due to influences from sensor calibration, solar angle, atmospheric scattering, and topographic shading, all of which are particularly relevant in the Santa-Babadjou Corridor's varied relief and seasonal climate. The electromagnetic radiation (EMR) reflected or emitted from land cover is altered by these factors before it reaches the satellite sensor. Therefore, preprocessing was conducted to minimize such distortions and obtain reliable surface reflectance data for land use/land cover and ecosystem service valuation [42].

In this study, we applied the COST model for radiometric correction [38] [39]. The COST model is image-based, requires no external atmospheric measurements, and effectively accounts for the multiplicative effects of atmospheric scattering and absorption. It has proven effective in tropical environments such as Cameroon, where seasonal haze and varying humidity can influence reflectance.

The radiometric correction process involved three main steps: (a) Conversion of DN values to spectral radiance at the sensor; (b) Conversion of spectral radiance to sensor reflectance; and (c) Atmospheric correction to derive surface reflectance from sensor reflectance. These steps were implemented in **R software** using the radCor() function of the **RStoolbox** package, ensuring consistent preprocessing across the time series of Landsat images for the Santa-Babadjou Corridor.

2.4. Classification of Land Use and Land Cover

The surface reflectance values obtained after radiometric and atmospheric correction in the preprocessing stage served as the basis for developing the LULC maps for the Santa-Babadjou Corridor. The classification process was performed using an unsupervised classification approach, which is well suited for capturing heterogeneous landscapes where natural, agricultural, and settlement areas are closely

interwoven. The Landsat images for each study year were classified into five primary LULC categories reflecting the major land cover features of the corridor and relevant to ecosystem service valuation: (a) Built-up area; (b) Vegetation-upland forest and grasslands; (c) Waterbody; (d) Agricultural land-cultivated fields. These categories align with biome-based classifications used in ecosystem service valuation studies, ensuring that the derived maps directly support the estimation of the changes in the corridor's ESVs over time. The definitions of each class are provided in **Table 2**.

Table 2. Description of Land use types.

Land Cover Type	*Description*
Built-up Area	Urban and developed areas, including residential, commercial, and industrial zones, settlements, transport infrastructure, and other man-made structures.
Waterbody	Natural or artificial water features such as rivers, lakes, ponds, canals, wetlands, and lowlands.
Vegetation	Areas dominated by trees, forests, gardens, parks, playgrounds, and natural green cover.
Bare Land	Land with little or no vegetation, including fallow land, construction sites, exposed soil, sand, and other barren surfaces.
Agricultural Land	Land used for farming activities, such as cropland, pasture, orchards, groves, and nurseries.

Since we used the unsupervised classification approach, the process was quick and straightforward, involving the generation of land cover classes based on the spectral characteristics of the satellite images without relying on visual interpretation [37]. In this approach, the analyst specifies the number of classes in advance, after which the software groups pixels with similar spectral properties into those predefined classes [43]. One limitation of unsupervised classification is that spectral reflectance values do not always align perfectly with distinct land cover categories, especially for pixels that have spectral characteristics similar to two adjacent classes. This often results in classification errors. To mitigate this, an iterative process to identify the optimal number of classes is necessary [37]. Several clustering algorithms exist for unsupervised classification, such as ISODATA, CLARA, mean-shift, agglomerative hierarchical clustering, PAM, random forest, and k-means clustering [44]. Among these, k-means clustering is widely used due to its simplicity, computational efficiency, robustness with high-dimensional spectral data, and effectiveness in classifying LULC. For this study, we applied the k-means algorithm in R software to classify the processed Landsat images into the five primary LULC classes relevant to the Santa-Babadjou Corridor [43].

The k-means algorithm partitions the data into a predefined number (k) of clusters by iteratively minimizing within-cluster variance while maximizing inter-

cluster differences [43]. A critical step in k-means classification is determining the optimal number of clusters, as this directly impacts classification accuracy. Several techniques exist for this purpose, including the elbow method, silhouette analysis, and gap statistics [42] [45]. Using the elbow method, which plots the explained variance against the number of clusters, we identified eight (8) as the optimal number of clusters for our spectral dataset. Since our classification scheme required five broad LULC categories, we initially ran the algorithm with $k = 8$ and subsequently regrouped the clusters into the five final classes consistent with the biome-based ESV framework (**Table 3**).

2.4.1. Filtering Techniques

The initial classified images exhibited 'salt-and-pepper' noise, a common artifact in medium-resolution satellite imagery like Landsat. Such noise and misclassification errors typically occur due to mixed pixels and spectral ambiguity. To enhance the classification results, a multi-step filtering procedure was adopted:

1) A 3 × 3 majority filter was applied using ArcGIS 10.8. This smoothing filter replaced each pixel's value with the majority value of its surrounding neighborhood, effectively reducing isolated spurious pixels.

2) The filtered raster was then converted to vector format, which allowed for manual correction of localized misclassification errors, particularly along settlement-farmland and forest-grassland boundaries where misclassification was most pronounced.

3) The cleaned and corrected data were then rasterized again to ensure consistency across datasets and to prepare them for subsequent change detection and ESV valuation [43].

This multi-step filtering significantly improved the spatial coherence of the LULC maps, reducing small-pixel misclassifications while preserving genuine landscape heterogeneity.

2.4.2. Accuracy Assessment Procedures

To ensure reliability, we conducted a rigorous accuracy assessment of the classified LULC maps. Reference data were obtained from high-resolution imagery available in Google Earth Pro and cross-checked with field knowledge from previous surveys in the Santa-Babadjou Corridor. For each classification year (1980, 1990, 2000, 2010, 2020, and 2024), a stratified random sampling of 250 - 300 validation points was performed. This approach ensured proportional representation across the five LULC classes, with oversampling of minority classes such as waterbodies and bare land to achieve adequate representation despite their limited spatial extent. **Table 1** shows the distribution of validation points across LULC classes for each year:

Each validation point was labeled using Google Earth imagery and corroborated with field knowledge, providing a reliable ground-truth dataset for comparison with the classified maps. Accuracy was quantified using a confusion matrix, from which the following metrics were derived:

Table 3. Distribution of validation points in the Santa-Babadjou corridor.

Year	Agriculture/Vegetation	Built-up	Bare Land	Waterbodies	Total Points
1980	140	50	30	30	250
1990	145	55	30	25	255
2000	150	55	35	30	270
2010	160	60	35	35	290
2020	150	35	25	20	280
2024	165	60	35	35	295

- **Overall Accuracy (OA):** the percentage of correctly classified pixels out of the total validation points.
- **User's Accuracy (UA):** the reliability that a pixel classified into a given category actually represents that category on the ground.
- **Producer's Accuracy (PA):** the probability that a reference pixel is correctly classified.
- **Kappa Coefficient (κ):** a statistic that accounts for chance agreement, widely used for LULC accuracy validation.

The results show that overall accuracies ranged from 85.60% (1980) to 91.00% (2024), while kappa coefficients varied between 0.758 and 0.865, demonstrating strong agreement between classification outputs and reference data. These values exceed the 85% threshold recommended by Anderson *et al.* (1976) for reliable LULC mapping. Beyond quantifying the LULC types, we analyzed their temporal changes throughout the study period, since LULC dynamics significantly affect ecosystem services and environmental functioning in the corridor. To quantify these changes, we employed the land-use dynamic index, calculated as shown in Equation (1) [46].

$$k = \frac{Aj - Ai}{Ai} x \frac{1}{T} x100 \quad (1)$$

where K represents the land-use dynamic index for a specific LULC type, Ai and Aj denote the initial and final areas of that LULC type, respectively, and T is the duration of the study period.

2.5. Assignment of Ecosystem Services Values

ESV has gained global attention as an important tool to understand the diverse benefits that ecosystems provide to human well-being. Over the past few decades, numerous studies have sought to estimate the economic value of ES, particularly focusing on tropical forests, endangered species management, and protected areas. Among the various valuation approaches, the model developed by Costanza is widely regarded as one of the most comprehensive and robust frameworks for estimating the economic value of ecosystem services [43]. [32] identified 17 ecosystem services across 16 biomes and used the benefit transfer method (BTM) to

estimate global economic values based on a synthesis of existing literature and original calculations. Since its introduction, this method has been extensively applied in diverse geographic contexts worldwide to assess ecosystem services.

While Costanza's model has faced some critiques, particularly regarding the potentially low valuation of farmland and uncertainties inherent in benefit transfer, it remains the most comprehensive initial approximation for ecosystem service valuation to date. Accordingly, we adopted this model to estimate ESVs for the Santa-Babadjou Corridor.

To assign ESVs to the five LULC categories identified in our study, we matched each LULC class with the most relevant biome category from [2] [44]. For instance, "cropland" was used as a proxy for "agricultural land", "wetland" for "waterbody", "tropical forest" for "forest and vegetation", and "urban" for "built-up area".

Although the alignment between LULC categories and Costanza's biomes is not exact, this proxy approach has been employed in many other ecosystem valuation studies [45]-[58]. The detailed correspondence between LULC types, equivalent biomes, and their associated ESV coefficients for the Santa-Babadjou Corridor is presented in **Table 4**.

Table 4. Biome equivalents for land-use categories and their corresponding ecosystem values.

LULC Types	*Equivalent Biome*	*ESV Coefficient* (*US* $ ha^{-1} yr^{-1})
Agricultural land	Cropland	92
Water body	Wetland	14,785
Forest and vegetation	Tropical forest	2007
Built-up area	Urban	0
Bare land	Desert	0

2.6. Determination of ESVs

Using the value coefficients from **Table 4**, the total ESVs were calculated by multiplying the land area by its corresponding VC, as shown in Equation (2).

$$\text{ESV} = \Sigma\ (A_K \times VC_k) \tag{2}$$

where ESV represents the total estimated value of ESs, A_k is the area in hectares, and VC_k is the value coefficient (US $ ha^{-1} yr^{-1}) for each LULC category k. To determine changes in ESV over time, we calculated the differences in the estimated ESV for each LULC category for the years 1980, 1990, 2000, 2010, 2020, and 2024. The rate of change in ESV was then computed using Equation (3).

$$ESV_{cr} = \frac{ESVj - ESVi}{ESVi} x \frac{1}{T} x100 \tag{3}$$

where ESV_{cr} denotes the annual *ESV* change rate for a specific LULC type, *ESVi* and *ESVj* are the initial and final ESVs, and T is the length of the study period. In

addition to calculating the ESV for each LULC category and assessing the impact of LULC changes on the total ESV, we also estimated the value of 17 ecosystem functions provided by each biome for the years 1980, 1990, 2000, 2010, 2020, and 2024 using Equation (4).

$$ESV_f = \Sigma\ (A_k \times VC_{fk}) \tag{4}$$

where ESV_f represents the estimated value of ecosystem service function f, Ak is the area (ha) of LULC category k, and VCfk is the value coefficient of function f (US \$ ha^{-1} yr^{-1}) for that LULC category. The VC for each individual function was derived from **Table 2** [43].

2.7. Determination of the Elasticity of Ecosystem Service Values from Land Use Land Cover Changes

Elasticity measures the responsiveness of one variable to changes in another. In this study, to understand how total ESV responds to changes in LULC, we calculated the elasticity of ESV with respect to LULC changes. This elasticity indicates the percentage change in ESV resulting from a percentage change in LULC. The calculation of ESV elasticity was carried out using Equations (5) and (6).

$$EEL = \frac{\frac{ESVj - ESVi}{ESVi} x \frac{1}{T} x100}{\text{LTP}}. \tag{5}$$

$$\frac{\sum_{n=1}^{n} \Delta LCAj - ESVi}{\sum_{n=1}^{n} LCAi} x \frac{1}{T} x100. \tag{6}$$

In the above equations, EEL represents the elasticity of total ESV with respect to LULC changes. ESV_a and ESV_e denote the initial and final ESVs, respectively, while T refers to the length of the study period. LTP indicates the percentage of land transition, reflecting the extent of LULC changes. ΔLCA_i represents the change in the area of LULC category *i* during the study period, and LCA_a is the total area of LULC category *i*.

2.8. Determination of Sensitivity Analysis

To determine the sensitivity of ESV changes in coefficient values assigned to each LULC category, we first conducted a milarity assessment between our five LULC categories and the sixteen biomes identified by [43]. The most similar biome was selected as a proxy for each LULC category. However, because these biomes do not perfectly correspond to the LULC categories, uncertainties exist in the coefficient values used for ESV calculation. Therefore, sensitivity analysis is crucial to assess how dependent the total ESV is on the coefficients of specific LULC types. The coefficient of sensitivity (CS) serves as a metric to verify how effectively the biomes represent the LULC categories and the accuracy of their associated VC. We applied the standard economic concept of elasticity to compute CS, as shown in Equation (7) [54] [59] [60].

$$CS = \frac{(ESVj - ESVi)/ESVi}{(VCjk - VCik)/VCik} \quad (7)$$

In this context, ESV and VC denote the estimated total ESV and the value coefficient, respectively; the subscripts *i* and *j* refer to the initial and adjusted values, while *k* designates the specific LULC category. To perform the sensitivity analysis, the VC for each LULC category was varied by ±50%, allowing the recalculation of the adjusted ESV and the coefficient of sensitivity (CS). By evaluating the CS, we can quantify how changes in the VC of a particular LULC type affect the total ESV. A CS value less than 1 indicates that the estimated ESV is inelastic relative to the VC, meaning it is relatively insensitive to such changes. Conversely, a CS greater than 1 suggests that the ESV is elastic and highly responsive to coefficient variations. When the ESV is inelastic with respect to the value coefficient, it implies that the chosen biome proxies and their associated ESV estimates are robust and reliable. Sensitivity analysis of this nature has been widely employed in previous studies to assess how fluctuations in VC impact ESV [37] [61].

3. Results

3.1. Land Use Land Cover Change

The spatial distribution and trends of land use and land cover (LULC) changes in the Santa-Babadjou Corridor from 1980 to 2024 are illustrated in **Figure 2**. In 1980, built-up areas were primarily concentrated in the center and southern part of the corridor. Over the subsequent decades, these built-up zones expanded in almost all directions, with notable growth occurring during the 1990s, 2000s, and 2010s. Agricultural land was predominantly located in the northern and northeastern sections in 1980. By 1990, parts of the forest cover in the west and northwest began to be converted into agricultural land, a trend that persisted through 2000 and 2010. However, between 2010 and 2024, much of this agricultural land was further transformed into built-up areas. Forests and grasslands, once largely concentrated in the western, northwestern, and eastern parts of the corridor in 1980, have been significantly reduced, with substantial portions replaced by expanding built-up and agricultural lands in each subsequent decade, particularly between 2000 and 2024.

The LULC results in **Figure 2(A)** illustrate that, in 1980, the corridor was predominantly covered by grasslands, occupying 38.3% (27,929.6 ha) of the area, followed closely by forests at 36.7% (26,783 ha). Farmlands accounted for 17.7%, reflecting an established agricultural presence, while settlements were limited to 6.1%, indicating a largely rural environment with scattered communities and minimal urban footprint.

By 1990 (**Figure 2(B)**), forest cover remained nearly stable at 36.7% (26,782.6 ha) but recorded a slight decline of -2.4%, signaling the beginning of deforestation pressures. Farmlands expanded significantly to 23.8% (+6.1%), largely through the conversion of forest and grassland areas, demonstrating intensifying agricultural activity. Grasslands decreased by 2.4%, while settlement areas remained

steady, reflecting minimal urban growth but sustained reliance on rural livelihoods.

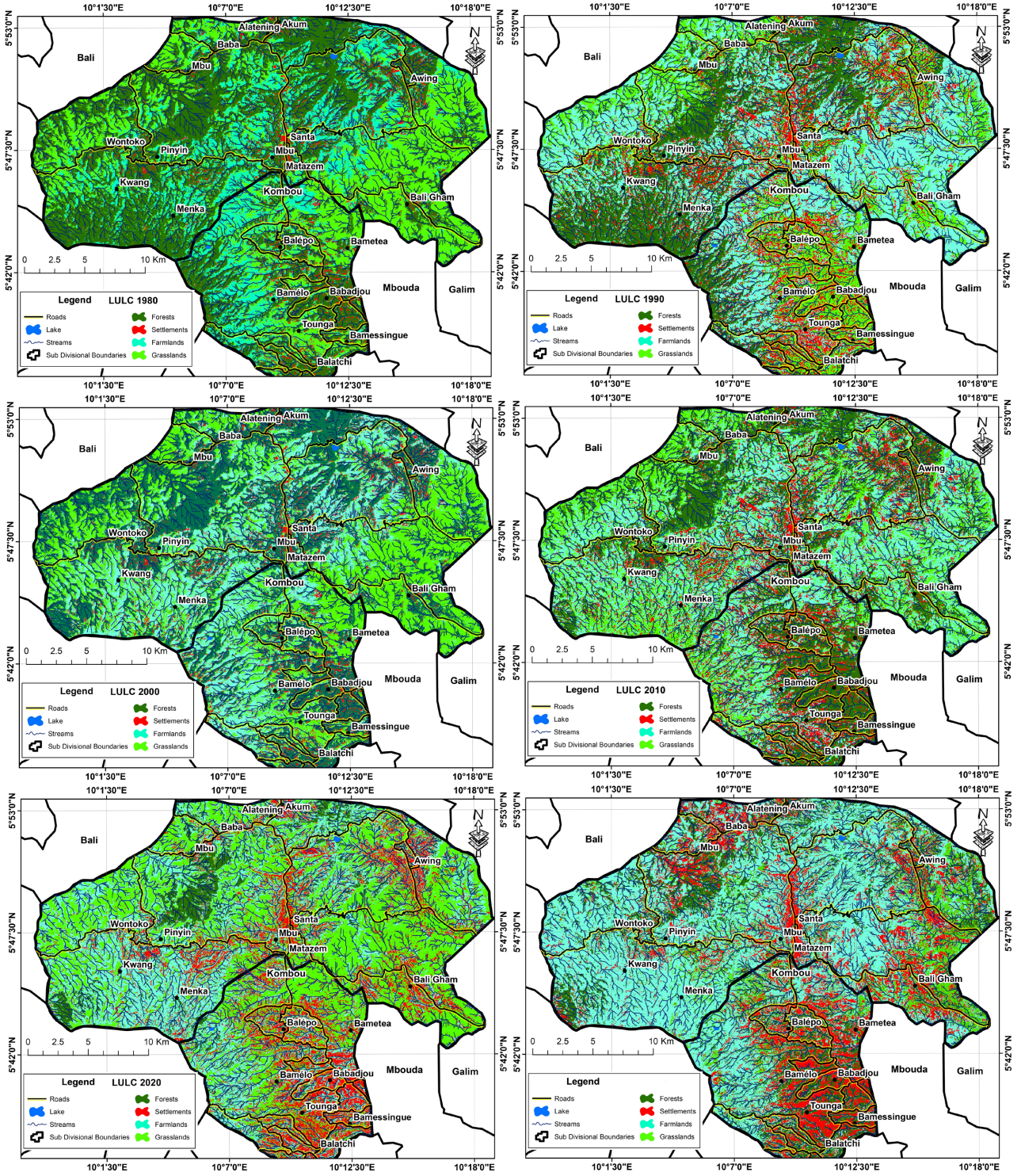

Figure 2. LULC change in Santa-Babadjou from 1980 to 2024.

In 2000 (**Figure 2(C)**), the corridor witnessed marked changes, with settlements

nearly doubling to 11.3% (+5.3%), highlighting the onset of urban expansion driven by infrastructural development and population shifts. Agricultural lands further increased to 26.4% (+2.7%), encroaching on natural landscapes. Forest cover declined by 2.8%, and grasslands contracted to 30.8%, illustrating continuing land conversion from natural to human-dominated uses.

The period between 2010 and 2015 (**Figure 2(D)**) saw accelerated transformations: settlements rose sharply to 19.4% (+8.1%), reflecting heightened development pressure and rural-to-urban migration. Farmlands surged to 34.6% (+8.2%), underscoring agriculture's growing economic importance. Forests decreased substantially by 12.9% to 30.9%, signaling rapid deforestation, while grasslands fell to 20.8%, reflecting diminished open spaces and grazing areas.

From 2015 to 2020 (**Figure 2(E)**), these trends intensified as the corridor's landscape shifted further under anthropogenic influence. Forests declined drastically to 15.8%, a reduction of nearly half over two decades. Settlements expanded to 22.1% (+2.7%), while grasslands dramatically dropped to 9.4% (−11.4%), indicating loss of natural vegetation and open land. Interestingly, farmlands slightly decreased to 35.5%, likely reflecting urban encroachment into agricultural zones.

By 2024 (**Figure 2(F)**), the cumulative impact of human activities was evident: forest cover shrank to 9.1% (−6.7%), the built-up area surged to 44.9%, nearly doubling in just four years, indicative of rapid urbanization. Farmlands dominated at 51.7%, illustrating the corridor's heavy dependence on agriculture for livelihoods and economic sustenance. Grasslands stabilized at 16.2%, though overall their reduction points to limited space for grazing or conservation. Water bodies remained marginal at 0.1%, showing negligible change. These shifts signal profound landscape transformation, with expanding settlements and farmland exerting pressure on ecological systems, water resources, and soil health, underscoring the urgent need for sustainable land management strategies.

The various LULC dynamics in the Santa-Babadjou Corridor have been quantified through percentage changes across different land use types, as presented in **Table 5**. By analyzing these multi-temporal changes, we gain crucial insights into how evolving human activities such as agricultural expansion, settlement growth, and fluctuations in grassland and forest cover reshape the landscape and alter the provision of ES. Understanding these shifts is vital for assessing changes in ESVs, as land cover changes directly impact the corridor's capacity to regulate hydrological processes, support biodiversity, and sustain local livelihoods. This analysis thus aligns closely with evaluating how land use dynamics influence surface and groundwater resources through their effect on ecosystem service provisioning.

The results in **Table 5** clearly illustrate that, from 1980 to 2024, the Santa-Babadjou corridor has experienced significant LULC transformations, indicating a progressive and often unsustainable transformation of its landscape. In 1980, the results in **Table 5** and **Figure 2** and **Figure 3** illustrate that built-up areas accounted for just 6.1% of the corridor, reflecting its largely rural character; however, steady increases through 1990 (6.3%), 2000 (11.3%), 2010 (18.0%), and 2020

(22.1%) culminated in an explosive expansion to 44.9% by 2024, driven by rapid urbanization, infrastructural development, and population growth. Forest cover, once the backbone of the corridor's ecology at 36.7% in 1980, remained relatively stable until 1990 (36.7%) before declining steadily to 33.9% (2000), 30.9% (2010), 15.8% (2020), and a mere 9.1% by 2024, marking a severe loss due to deforestation and land conversion. Farmland expanded consistently, rising from 17.7% in 1980 to 23.8% (1990), 26.4% (2000), 34.6% (2010), 35.5% (2020), and peaking at 51.7% by 2024, underscoring agricultural intensification as a primary driver of land transformation. Grasslands, the dominant cover in 1980 at 38.3%, saw a steady decline to 35.9% (1990), 30.8% (2000), 20.8% (2010), 9.4% (2020), before stabilizing slightly at 16.2% in 2024, much of this area having been converted to farmland or urban space. Waterbodies remained negligible throughout the period, consistently around 0.1%, indicating minimal hydrological surface change. Collectively, these trends show a clear pattern of expanding settlements and agriculture at the expense of forests and grasslands, with direct implications for biodiversity loss, soil degradation, and altered hydrological processes.

Table 5. Land cover/land use practices in the Santa-Babadjou corridor.

1980	Class_Name	Area	Percentage	% difference 1980-1990
1	Forests	26783.0	36.7	0.0
2	Settlements	4430.0	6.1	0.0
3	Farmlands	12918.1	17.7	6.1
4	Grasslands	27929.6	38.3	−2.4
1990	Class_Name	Area	Percentage	% difference 1990-2000
1	Forests	26782.6	36.7	−2.4
2	Settlements	4429.9	6.1	−12.4
3	Farmlands	17319.1	23.8	2.7
4	Grasslands	26243.3	36.0	−5.2
2000	Class_Name	Area	Percentage	% difference 2000-2005
1	Forests	25034.1	34.3	−2.8
2	Settlements	8262.4	11.3	5.3
3	Farmlands	19276.0	26.4	2.7
4	Grasslands	22446.5	30.8	−5.2
2010	Class_Name	Area	Percentage	% difference 2010-2015
1	Forests	22562.0	30.9	−12.9
2	Settlements	14141.7	19.4	1.4
3	Farmlands	25221.8	34.6	6.2
4	Grasslands	15192.8	20.8	−4.5
5	Lake	64.2	0.1	0.1

Continued

2020	Class_Name	Area	Percentage	% difference 2020-2024
1	Forests	11526.9	15.8	−6.7
2	Settlements	16084.5	22.1	22.8
3	Farmlands	25916.4	35.5	16.1
4	Grasslands	6849.6	9.4	−6.3
5	Lake	64.2	0.1	0.1
2024	Class_Name	Area	Percentage	% difference 2024-2025
1	Forests	6620.7	9.1	−1.1
2	Settlements	32708.0	44.9	0.3
3	Farmlands	37694.5	51.7	−21.2
4	Grasslands	11848.3	16.2	−13.1
5	Lake	64.2	0.1	0

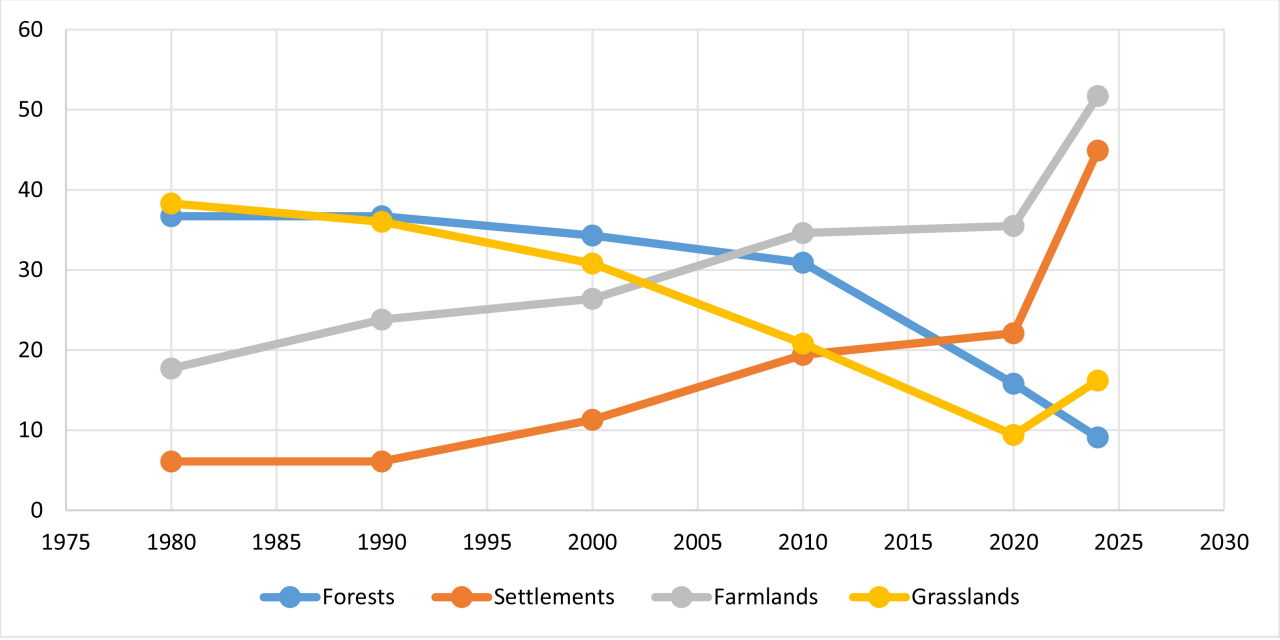

Figure 3. Land use land cover changes in the Santa-Babadjou corridor from 1980 to 2024.

3.2. Variation in Ecosystem Services Value

3.2.1. Change in Ecosystem Services Value

We estimated the ESV of the Santa-Babadjou corridor for each LULC type using Equation (2) and the ESV coefficients presented in **Table 6**.

The ES results in **Table 6** show that the Santa-Babadjou corridor has undergone a sustained decline in ESV, falling from US$220.12 million in 1980 to US$33.70 million by 2024, an 85% reduction that reflects deep environmental degradation. The decline was relatively modest in the first three decades, dropping from US$220.12 M in 1980 to US$213.50 M in 1990, then to US$191.22 M in 2000, and

US$183.47 M in 2005. The downward trend in ESV intensified after 2010, with ESV dropping to US$152.15 M that year, then to US$75.53 M in 2020, and collapsing to US$33.70 M by 2025, indicating a phase of accelerated ecosystem stress. At the center of this collapse are forests and grasslands, which together contributed almost 99% of total ESV in 1980: US$101.78 M from 26,783 ha of forest and US$116.35 M from 27,930 ha of grassland. Their coverage remained largely stable between 1980 and 1990 (forest: 26,782 ha, US$101.77 M; grassland: 26,243 ha, US$109.33 M) before declining steeply. By 2000, forest area had reduced to 25,034 ha (US$95.13 M) and grasslands to 22,447 ha. The degradation gained steam over the next two decades, with forest area dropping to 11,527 ha (US$43.80 M) and grasslands to 6,850 ha (US$28.54 M) by 2020, collapsing further to 5,783 ha (US$21.97 M) and 2,265 ha (US$9.44 M) respectively by 2024. These losses have critically weakened the corridor's ecological backbone, eroding biodiversity, destabilizing watersheds, and other key hydrological processes.

Table 6. Evolution of ecosystem services in the Santa-Babadjou corridor.

LU Class	LU (Ha)	1980 ES Coefficient (US$ Ha^{-1}/y)	Estimated ESV	
Forests	26,783	3800	101775400.0	101.78
Farmlands	12918.1	92	1188465.2	1.19
Grasslands	27929.6	4166	116354713.6	116.35
lake	64.2	12,512	803270.4	0.80
				220.12
LU Class	LU (Ha)	1990	Estimated ESV	
Forests	26782.6	3800	101773880	101.77
Farmlands	17319.1	92	1593357.2	1.59
Grasslands	26243.3	4166	109329587.8	109.33
lake	64.2	12,512	803270.4	0.80
				213.50
LU Class	LU (Ha)	2000	Estimated ESV	
Forests	25034.1	3800	95129580	95.13
Farmlands	19276	92	1773392	1.77
Grasslands	22446.5	4166	93512119	93.51
lake	64.2	12512	803270.4	0.80
				191.22
LU Class	LU (Ha)	2010	Estimated ESV	
Forests	22562	3800	85735600	85.74
Farmlands	25221.8	92	2320405.6	2.32
Grasslands	15192.8	4166	63293204.8	63.29
lake	64.2	12,512	803270.4	0.80
				152.15

Continued

LU Class	LU (Ha)	2020	*Estimated ESV*	
Forests	11526.9	3800	43802220	43.80
Farmlands	25916.4	92	2384308.8	2.38
Grasslands	6849.6	4166	28535433.6	28.54
lake	64.2	12,512	803270.4	0.80
				75.53
LU Class	LU (Ha)	2024	Estimated ESV	
Forests	5782.6	3800	21973880	21.97
Farmlands	22261.8	92	2048085.6	2.05
Grasslands	2265.4	4166	9437656.4	9.44
lake	19.3	12,512	241481.6	0.24
				33.70

On the other hand, other land use changes have exerted additional pressure on the ecosystem. Farmlands have expanded from 12,918 ha (US$1.19 M) in 1980 to 17,319 ha in 1990 (US$1.59 M), 19,276 ha in 2000 (US$1.77 M), and peaked at 25,916 ha in 2020 (US$2.38 M) before declining slightly to 22,262 ha (US$2.05 M) in 2024. Built-up areas have grown from 4430 ha in 1980 to 8,262 ha in 2000, doubling to 16,085 ha in 2020, and 32,924 ha in 2024. Although settlements contribute no direct ESV due to their coefficient value of zero, their expansion has been a major driver of habitat loss, ecosystem fragmentation, and land conversion. Waterbodies, like Lake Awing, have also suffered significant contraction, shrinking from 64.2 ha (US$0.80 M) in 1980 to just 19.3 ha in 2024, with a corresponding loss of US$0.24 M in value, indicating a marked decline in aquatic ecosystem health.

The annual percentage change analysis in **Figure 4** further reveals severe erosion of ecosystem services across the Santa-Babadjou corridor, driven primarily by the land-use transitions in **Figures 2(A-F)**. Forests show sustained and substantial losses, with the steepest drop of −US$35.66 million recorded between 2010 and 2015, reflecting intensified deforestation, while grasslands display even greater declines, experiencing sharp declines of −US$30.22 million between 2005 and 2010 and a significant −US$39.92 million between 2024 and 2025, indicating accelerated ecosystem degradation. Farmlands present a mixed pattern with occasional gains of +US$1.08 million from 2020 to 2024.

Collectively, the ESV shifts in figure 4 illustrate that rapid urbanization, farmland expansion, and the degradation of forests and grasslands have jointly dismantled the corridor's natural capital, highlighting the urgent need for integrated policy interventions to halt further declines, restore degraded ecosystems, and safeguard the services essential for environmental resilience and community well-being.

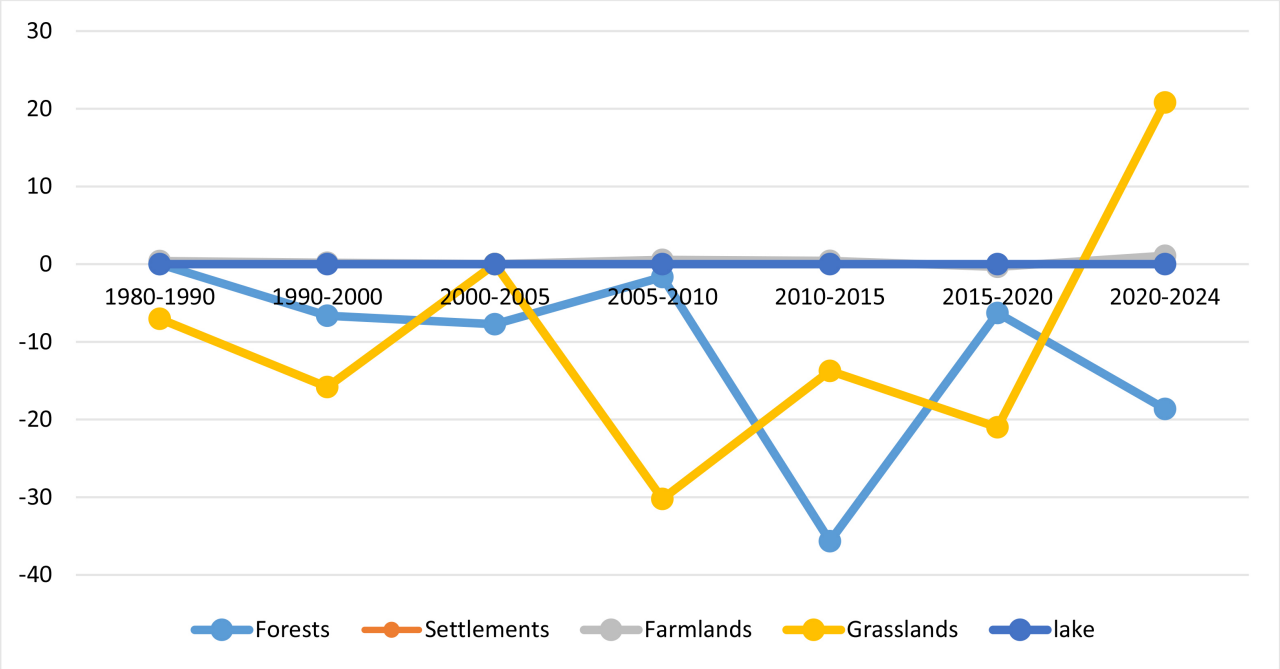

Figure 4. Annual evolution of ecosystem service values in the Santa-Babadjou corridor.

3.2.2. Estimation of the Value of Individual Ecosystem Service Function

In this study, as presented in Table 6, the value of 17 individual ecosystem functions within the Santa-Babadjou Corridor was estimated using Equation (4), the spatial extent of each LULC type derived for the study area (Figure 3), and the value coefficients for individual ecosystem functions provided in Table 2. Furthermore, we examined how LULC changes in the corridor influenced variations in each ecosystem function over the period 1980-2024. The estimated values for the 17 ecosystem functions are presented in Table 7. These functions are grouped into four broad categories: provisioning, regulating, supporting, and cultural services. Quantifying the value of each function provides a clear understanding of its relative contribution to the overall ESV of the Santa-Babadjou Corridor.

The results in Table 7 illustrate that all four ecosystem service categories—Provisioning, Regulating, Supporting, and Cultural—have experienced significant declines across the Santa-Babadjou Corridor between 1980 and 2024. These losses are strongly linked to widespread land use and land cover changes, critically impacting the valuation, availability, and sustainability of surface and groundwater resources.

Figure 5(A) illustrates that provisioning services, including food, raw materials, and water supply, fell sharply from US$108.2 million in 1980 to US$58.8 million in 2024. Water supply alone decreased from US$12.5 million to US$7.5 million, reflecting degradation of aquifer recharge zones and riparian buffers. Native upland forests shrank from 36.7% (2678 ha) in 1980 to 9.1% (1600.7 ha) in 2024, while Eucalyptus plantations expanded from 0.4% (32.6 ha) to 11.6% (849.1 ha), undermining groundwater reliability and increasing water collection times.

Table 7. Evolution of ecosystem service functions in the Santa-Babadjou corridor.

Serial No		ESV functions							
Provisioning		1980	1990	2000	2005	2010	2015	2020	2024
1	Food production	36.3	35.1	30.1	27.9	25.6	23.7	21.8	19.9
2	Raw materials	11.0	10.6	9.1	8.3	7.5	6.9	6.3	5.6
3	Genetic resources	48.4	46.8	40.0	37.0	34.1	31.5	29.0	26.4
4	Water supply	12.5	12.1	10.3	9.6	8.8	8.1	7.5	6.8
Total		108.2	104.6	89.5	82.7	76.0	70.2	64.5	58.8
		Regulating							
5	Gas regulation	18.1	17.5	14.9	13.8	12.7	11.7	10.8	9.9
6	Disturbance regulation	1.3	1.2	1.1	1.0	0.9	0.8	0.8	0.7
7	Erosion control	7.3	7.1	6.1	5.6	5.2	4.8	4.4	4.0
8	Pollination	1.1	1.1	0.9	0.9	0.8	0.7	0.7	0.6
9	Climate regulation	48.0	46.1	39.8	36.8	33.9	31.1	28.2	25.4
10	Biological control	11.8	11.3	10.0	9.3	8.5	7.8	7.1	6.4
11	Water regulation	1.9	1.8	1.6	1.5	1.4	1.2	1.1	1.0
12	Waste-treatment	0.8	0.8	0.6	0.6	0.5	0.5	0.5	0.4
Total		90.2	86.8	74.1	68.7	63.8	58.7	53.5	48.4
		Supporting							
13	Nutrient cycling	4.4	4.3	3.6	3.4	3.1	2.9	2.6	2.3
14	Soil formation	1.0	0.9	0.8	0.7	0.7	0.6	0.6	0.5
15	Habitat/refugia	59.8	57.5	48.6	44.6	40.6	37.3	33.9	30.5
Total		65.2	62.7	53.0	48.7	44.4	40.7	37.1	33.4
		Cultural							
16	Cultural	2.6	2.5	2.2	2.0	1.8	1.7	1.5	1.4
17	Recreation	66.4	63.8	54.4	50.5	46.7	42.8	38.9	35.1
Total		69.0	66.3	57.0	52.5	48.5	44.5	41.2	36.5

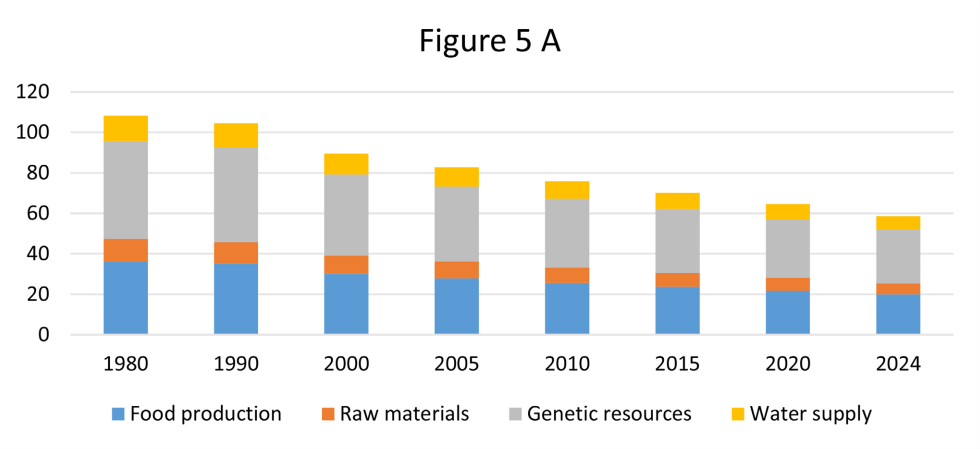

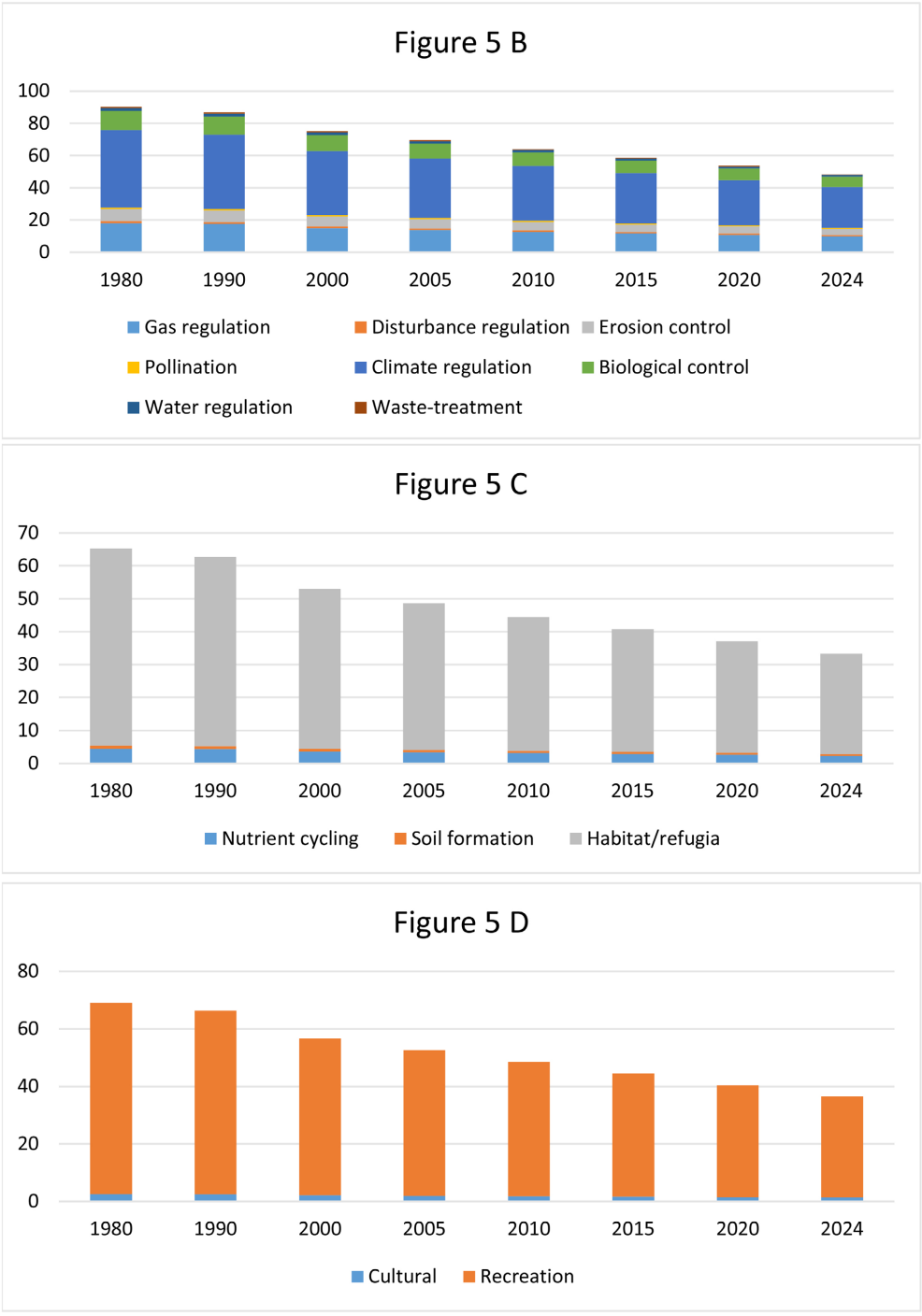

Figure 5. Contribution of individual ecosystem services to total ESV in the Santa-Babadjou corridor.

Furthermore, the results in **Figure 5(B)** also revealed that regulating services declined from US$90.2 million in 1980 to US$53.5 million in 2024. Specifically, gas and climate regulation values were reduced by half from US$66.1 million to US$33.5 million. In addition, erosion control dropped from US$7.3 million to US$3.8 million. Moreover, declines in waste treatment services have contributed to poorer water quality and increased waterborne diseases. Supporting services

(Figure 5(C)) also decreased from US$65.2 million in 1980 to US$37.1 million in 2024; within this category, habitat provision fell from US$59.8 million to US$28.2 million, reflecting the loss of critical recharge areas and biodiversity. Simultaneously, nutrient cycling impairment has increased runoff pollution and water contamination across all sub-watersheds. Meanwhile, cultural services (Figure 5(D)) dropped from US$69.0 million in 1980 to US$41.2 million in 2024, with recreational values reduced from US$66.4 million to US$32.4 million, as degradation and drying of water bodies reduced cultural significance, tourism potential, and community support for conservation efforts.

The ESV results in Table 7 and Figure 5 clearly illustrate that the ESV in the corridor has been on a steady decline. This is further depicted in Figure 6, which shows the cumulative effect of LULC changes on the total ESV for each of the functions presented in Table 7. Provisioning services dropped from US$108.2 million in 1980 to US$58.8 million in 2024, reflecting significant reductions in resources such as water supply and raw materials. Regulating services declined from US$90.2 million to US$48.4 million, indicating reduced capacity for climate regulation, erosion control, and waste treatment. Supporting services fell from US$65.2 million to US$33.4 million, signaling habitat loss and nutrient cycling disruption. Cultural services decreased from US$69.0 million to US$36.5 million, pointing to reduced recreational and heritage values.

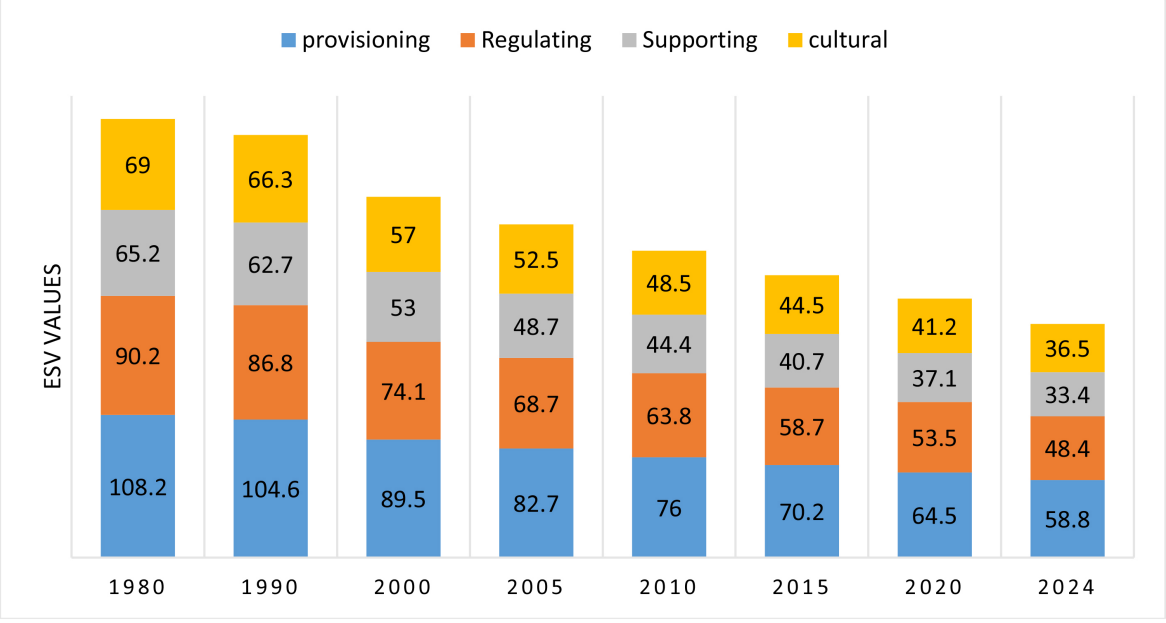

Figure 6. Effects of land use land cover change on the different ecosystem service functions in the corridor.

4. Discussion

4.1. Land Use Land Cover Change Dynamics

This study quantifies the dynamics of LULC change and their impacts on ESs in the study Santa-Babadjou corridor from 1980 to 2024 [62] [63]. The results indi-

cate significant shifts across all major LULC classes [38] [39] [64]. Forest cover decreased from 26783.0 ha (36.7%) in 1980 to just 6620.7 ha (9.1%) in 2024, reflecting a total decline of 75.3% [65]. Grasslands followed a similar downward trend, shrinking from 27929.6 ha (38.3%) to 11848.3 ha (16.2%), amounting to a 57.6% reduction [61] [65]. Farmlands fluctuated but ultimately fell from 19118.1 ha (23.8%) to 11950.4 ha (16.4%), a 37.5% decrease [66]. Conversely, settlement areas expanded dramatically from 4430.0 ha (6.1%) in 1980 to 32709.5 ha (44.9%) in 2024, representing a 638.6% increase, largely at the expense of forests, farmlands, and grasslands [66]. Lakes remained a minor class throughout the period, with only slight fluctuations around 64 ha. The observed LULC changes are both dynamic and nonlinear, driven by multiple interacting factors [38] [40] [41]. The unprecedented expansion of settlements is closely linked to rapid urbanization, infrastructural development, and population growth in the corridor [39], which have accelerated the conversion of natural and semi-natural landscapes into built-up areas [66] [67]. This conversion has been fueled by increased demand for housing, agriculture, service facilities, and transport infrastructure [61] [68]. The loss of forests and grasslands has reduced biodiversity habitats and carbon regulation capacity [69], while farmland decline threatens local food security. The reduced vegetation cover has also increased vulnerability to soil erosion [70], altered hydrological patterns [40], and exacerbated the risk of flooding in low-lying areas [39] [71]. These changes illustrate a profound transformation of the landscape, where human-driven LULC conversion is reshaping the ecological and socioeconomic character of the corridor.

4.2. Assessment of Ecosystem Service Values

Based on the observed LULC changes, we quantified the ESV of the Santa-Babadjou corridor for the period from 1980 to 2024. Our findings confirm that LULC change is a key driver of shifts in ecosystem services in the region [72] [73]. However, due to differences in value coefficients and the extent of each land class, the magnitude of impact on ESV varied greatly across LULC categories [66] [69].

The total ESV of the Santa-Babadjou corridor in 1980 was estimated at 220.12 million USD, dominated by contributions from grasslands (116.35 million USD) and forests (101.78 million USD) [1] [74]. By 1990, the total ESV had slightly declined to 213.50 million USD, driven mainly by decreases in grasslands (109.33 million USD) and farmlands (1.59 million USD), while forests remained stable at around 101.77 million USD [75] [76].

From 2000 onward, the rate of ESV decline accelerated. In 2000, the total ESV was 191.22 million USD, with forest value falling to 95.13 million USD and grassland value to 93.51 million USD [71]. By 2010, the total ESV had dropped to 152.15 million USD, largely due to the sharp reduction in grasslands (63.93 million USD) and forest cover (85.76 million USD). Similar sharp declines in forest and grassland contributions to ecosystem services have been observed in other African highland studies [77].

Between 2010 and 2020, the decline became even steeper. Forest ESV fell to 43.28 million USD, grasslands to 28.54 million USD, and the total corridor ESV reached 75.53 million USD [78] [79]. By 2024, the ESV reached its lowest point in the 44-year record, 33.70 million USD, with forests contributing just 2.20 million USD and grasslands 9.97 million USD.

Farmland ESV, although never a major contributor, also declined from 1.19 million USD in 1980 to 2.05 million USD in 2024 after some fluctuations, while lakes remained a consistently minor class, peaking at 0.80 million USD in the earlier years and falling to 0.24 million USD by 2024.

On the whole, the Santa-Babadjou corridor experienced an 84.7% reduction in total ESV from 1980 to 2024. This trend closely mirrors the extensive loss of forest and grassland cover documented in our LULC analysis [61] [64] [65] [69] [80], and is consistent with findings from other peri-urbanizing regions where settlement growth has displaced natural and semi-natural landscapes. Since built-up land yields no ESV, its expansion from a marginal class in 1980 to a dominant feature by 2024 has been a major factor in the collapse of ecosystem service provision in the region.

In terms of individual ecosystem service functions, regulating services (largely supported by forest and grassland cover) consistently represented the largest share of ESV in the early decades, but their contribution diminished drastically as vegetation cover was replaced by urban and peri-urban developments. Provisioning services, such as food and raw material supply from farmlands, also contracted over time, while the water-related services of lakes, though small in area, showed the highest per-hectare value but minimal influence on total ESV due to their limited extent [72] [81].

5. Conclusion

This study analyzes how ESV (ESV) in the Santa-Babadjou corridor changed between 1980 and 2024 due to land use and land cover (LULC) transformations. Over the period, settlement area expanded from 4,430.0 ha (6.1%) to 32,709.5 ha (44.9%), an increase of 638.6%, replacing forests, grasslands, and farmlands. Forest cover declined by 75.3%, grasslands by 57.6%, and farmlands by 37.5%, largely due to rapid urbanization, population growth, and infrastructure development. The total ESV dropped from 220.12 million USD in 1980 to 33.70 million USD in 2024, a decline of 84.7%. The sharpest fall occurred between 2010 and 2020, when ESV decreased by 50.3%, driven by losses in regulating and provisioning services. Forest ESV fell from 101.78 million USD to 2.20 million USD, and grasslands from 116.35 million USD to 9.97 million USD. Farmland ESV also declined, while lakes, though valuable per hectare, remained too limited to offset losses. The loss of vegetation cover has reduced biodiversity, increased soil erosion risk, altered hydrological cycles, and weakened climate regulation. These findings highlight the urgent need for integrating ecosystem service valuation into land-use planning to balance development with conservation and sustain the region's ecological and

socioeconomic health.

Conflicts of Interest

The authors declare no conflicts of interest regarding the publication of this paper.

References

[1] Bigirwa, D., Philip, D. and Mombo, F. (2025) Economic Valuation of Natural Water Purification Services: Addressing the Undervaluation of Non-Marketed Water Ecosystem Services in Tanzania's Lower Rufiji Sub-Basin. *Journal of Environmental Management*, **392**, Article ID: 126805. https://doi.org/10.1016/j.jenvman.2025.126805

[2] Chen, H. and Costanza, R. (2024) Valuation and Management of Desert Ecosystems and Their Services. *Ecosystem Services*, **66**, Article ID: 101607. https://doi.org/10.1016/j.ecoser.2024.101607

[3] Costanza, R. (2024) Misconceptions about the Valuation of Ecosystem Services. *Ecosystem Services*, **70**, Article ID: 101667. https://doi.org/10.1016/j.ecoser.2024.101667

[4] Khan, S.U., Guo, X., Hu, J., Khan, A.A., Talpur, M.A., Liu, G., *et al.* (2022) Who Cares and How Much? Narrative for Advances in Aquatic Ecosystem Services through Non-Market Valuation with Spatial Dimensions Using a Discrete Choice Experiment. *Journal of Cleaner Production*, **337**, Article ID: 130603. https://doi.org/10.1016/j.jclepro.2022.130603

[5] Taffarello, D., Bittar, M.S., Sass, K.S., Calijuri, M.C., Cunha, D.G.F. and Mendiondo, E.M. (2020) Ecosystem Service Valuation Method through Grey Water Footprint in Partially-Monitored Subtropical Watersheds. *Science of the Total Environment*, **738**, Article ID: 139408. https://doi.org/10.1016/j.scitotenv.2020.139408

[6] Stoeckl, N., Costanza, R., Dorji, N., Kubiszewski, I., Limenih, B., Tian, J., *et al.* (2025) Valuing the Reciprocating Services That Humans Can Provide to Ecosystems. *Ecological Indicators*, **174**, Article ID: 113496. https://doi.org/10.1016/j.ecolind.2025.113496

[7] Gao, F., Zhou, J., Jiang, H., Yang, W. and Wang, G. (2024) Assessing the True Value of Ecological Restoration in Mining Areas: An Input-Output Approach Based on Ecosystem Service Valuation. *Ecological Indicators*, **166**, Article ID: 112591. https://doi.org/10.1016/j.ecolind.2024.112591

[8] Hackbart, V.C.S., de Lima, G.T.N.P. and dos Santos, R.F. (2017) Theory and Practice of Water Ecosystem Services Valuation: Where Are We Going? *Ecosystem Services*, **23**, 218-227. https://doi.org/10.1016/j.ecoser.2016.12.010

[9] Hatan, S., Fleischer, A. and Tchetchik, A. (2021) Economic Valuation of Cultural Ecosystem Services: The Case of Landscape Aesthetics in the Agritourism Market. *Ecological Economics*, **184**, Article ID: 107005. https://doi.org/10.1016/j.ecolecon.2021.107005

[10] Kang, N., Hou, L., Huang, J. and Liu, H. (2022) Ecosystem Services Valuation in China: A Meta-Analysis. *Science of the Total Environment*, **809**, Article ID: 151122. https://doi.org/10.1016/j.scitotenv.2021.151122

[11] Acharya, R.P., Maraseni, T. and Cockfield, G. (2019) Global Trend of Forest Ecosystem Services Valuation—An Analysis of Publications. *Ecosystem Services*, **39**, Article ID: 100979. https://doi.org/10.1016/j.ecoser.2019.100979

[12] Amirnejad, H., Hosseini, S. and Azadi, H. (2025) Evaluation and Valuation of Tajan River Basin Ecosystem Services. *Ecohydrology & Hydrobiology*, **25**, 238-249.

https://doi.org/10.1016/j.ecohyd.2024.03.005

[13] Primmer, E. and Furman, E. (2024) How Have Measuring, Mapping and Valuation Enhanced Governance of Ecosystem Services? *Ecosystem Services*, **67**, Article ID: 101612. https://doi.org/10.1016/j.ecoser.2024.101612

[14] Spence, D.S., Baulch, H.M. and Lloyd-Smith, P. (2023) Collaborative Valuation of Ecosystem Services to Inform Lake Remediation. *Environmental Science & Policy*, **150**, Article ID: 103595. https://doi.org/10.1016/j.envsci.2023.103595

[15] Albaladejo-García, J.A., Alcon, F., Martínez-Carrasco, F. and Martínez-Paz, J.M. (2023) Understanding Socio-Spatial Perceptions and Badlands Ecosystem Services Valuation. Is There Any Welfare in Soil Erosion? *Land Use Policy*, **128**, Article ID: 106607. https://doi.org/10.1016/j.landusepol.2023.106607

[16] Aryal, K., Ojha, B.R. and Maraseni, T. (2021) Perceived Importance and Economic Valuation of Ecosystem Services in Ghodaghodi Wetland of Nepal. *Land Use Policy*, **106**, Article ID: 105450. https://doi.org/10.1016/j.landusepol.2021.105450

[17] Bélisle, A.C., Wapachee, A. and Asselin, H. (2021) From Landscape Practices to Ecosystem Services: Landscape Valuation in Indigenous Contexts. *Ecological Economics*, **179**, Article ID: 106858. https://doi.org/10.1016/j.ecolecon.2020.106858

[18] Dai, P., Zhang, S., Gong, Y., Zhou, Y. and Hou, H. (2022) A Crowd-Sourced Valuation of Recreational Ecosystem Services Using Mobile Signal Data Applied to a Restored Wetland in China. *Ecological Economics*, **192**, Article ID: 107249. https://doi.org/10.1016/j.ecolecon.2021.107249

[19] Fleischer, A., Gindin, Y. and Tsur, Y. (2025) Integrating Recreational Ecosystem Service Valuations into Israel's Water Economy. *Ecological Economics*, **227**, Article ID: 108391. https://doi.org/10.1016/j.ecolecon.2024.108391

[20] Azadi, H., Van Passel, S. and Cools, J. (2021) Rapid Economic Valuation of Ecosystem Services in Man and Biosphere Reserves in Africa: A Review. *Global Ecology and Conservation*, **28**, e01697. https://doi.org/10.1016/j.gecco.2021.e01697

[21] Cubillo, A.M., Lopes, A.S., Ferreira, J.G., Moore, H., Service, M. and Bricker, S.B. (2023) Quantification and Valuation of the Potential of Shellfish Ecosystem Services in Mitigating Coastal Eutrophication. *Estuarine, Coastal and Shelf Science*, **293**, Article ID: 108469. https://doi.org/10.1016/j.ecss.2023.108469

[22] Fassina, C., Jarvis, D., Tavares, S. and Coggan, A. (2022) Valuation of Ecosystem Services through Offsets: Why Are Coastal Ecosystems More Valuable in Australia than in Brazil? *Ecosystem Services*, **56**, Article ID: 101449. https://doi.org/10.1016/j.ecoser.2022.101449

[23] Aznarez, C., Pacheco, J.P., Domínguez, M.C., Gadino, I., Inda, H. and Castellarini, F. (2025) Green Gentrification Drives Socio-Cultural Shifts from Provisioning to Cultural Valuation of Ecosystem Services. *Ecosystem Services*, **73**, Article ID: 101731. https://doi.org/10.1016/j.ecoser.2025.101731

[24] Garrido Mateos, L., Rodríguez-López, F. and Sánchez-Macías, J.I. (2025) The Three-Stage Evolution in the Economic Valuation of Nature: Externalities, Ecosystem Services, and Natural Capital Accountability. *Journal of Cleaner Production*, **518**, Article ID: 145899. https://doi.org/10.1016/j.jclepro.2025.145899

[25] Barbier, E.B. (2016) The Protective Service of Mangrove Ecosystems: A Review of Valuation Methods. *Marine Pollution Bulletin*, **109**, 676-681. https://doi.org/10.1016/j.marpolbul.2016.01.033

[26] Bronzes, A., Hein, L., Groeneveld, R. and Pulatov, A. (2025) A Comparison of Valuation Methods for Cultural Ecosystem Services in Support of Ecosystem Accounting.

One Ecosystem, **10**, e108556. https://doi.org/10.3897/oneeco.10.e108556

[27] Chen, H. (2020) Land Use Trade-Offs Associated with Protected Areas in China: Current State, Existing Evaluation Methods, and Future Application of Ecosystem Service Valuation. *Science of the Total Environment*, **711**, Article ID: 134688. https://doi.org/10.1016/j.scitotenv.2019.134688

[28] Hattam, C., Böhnke-Henrichs, A., Börger, T., Burdon, D., Hadjimichael, M., Delaney, A., *et al.* (2015) Integrating Methods for Ecosystem Service Assessment and Valuation: Mixed Methods or Mixed Messages? *Ecological Economics*, **120**, 126-138. https://doi.org/10.1016/j.ecolecon.2015.10.011

[29] Morando-Figueroa, C.Z., Salazar-Briones, C., Ruiz-Gibert, J.M. and Lomelí-Banda, M.A. (2023) Ecosystem Services Valuation in Developing Countries: A Review of Methods and Applicability Approach. *Proceedings of the Institution of Civil Engineers—Urban Design and Planning*, **176**, 6-22. https://doi.org/10.1680/jurdp.21.00045

[30] Schmidt, K., Walz, A., Martín-López, B. and Sachse, R. (2017) Testing Socio-Cultural Valuation Methods of Ecosystem Services to Explain Land Use Preferences. *Ecosystem Services*, **26**, 270-288. https://doi.org/10.1016/j.ecoser.2017.07.001

[31] Vo, Q.T., Kuenzer, C., Vo, Q.M., Moder, F. and Oppelt, N. (2012) Review of Valuation Methods for Mangrove Ecosystem Services. *Ecological Indicators*, **23**, 431-446. https://doi.org/10.1016/j.ecolind.2012.04.022

[32] Costanza, R., d'Arge, R., de Groot, R., Farber, S., Grasso, M., Hannon, G., *et al.* (1996) The Value of the World's Ecosystem Services and Natural Capital. *Nature*, **387**, 253-260.

[33] Chen, H. (2020) Complementing Conventional Environmental Impact Assessments of Tourism with Ecosystem Service Valuation: A Case Study of the Wulingyuan Scenic Area, China. *Ecosystem Services*, **43**, Article ID: 101100. https://doi.org/10.1016/j.ecoser.2020.101100

[34] Awazi, N.P., Tientcheu-Avana, M., Temgoua, L.F., Tsufac, A.R., Forje, G.W., Cedric, C.D., *et al.* (2024) Agroforestry-Based Bioeconomy Transition in Cameroon: Realities and the Way Forward. In: Singh, K., Ribeiro, M.C. and Calicioglu, Ö., Eds., *Biodiversity and Bioeconomy*, Elsevier, 295-324. https://doi.org/10.1016/b978-0-323-95482-2.00014-6

[35] Zangmo Tefogoum, G., Kagou Dongmo, A., Nkouathio, D.G. and Gountié Dedzo, M. (2022) The Geodiversity of Lefo and Santa-Mbu Calderas (Bamenda Mountains, Cameroon Volcanic Line): Factor for Socioeconomic Activities. *International Journal of Geoheritage and Parks*, **10**, 491-506. https://doi.org/10.1016/j.ijgeop.2022.08.009

[36] Saha, S., Bera, B., Shit, P.K., Bhattacharjee, S. and Sengupta, N. (2022) Estimation of Carbon Budget through Carbon Emission-Sequestration and Valuation of Ecosystem Services in the Extended Part of Chota Nagpur Plateau (India). *Journal of Cleaner Production*, **380**, Article ID: 135054. https://doi.org/10.1016/j.jclepro.2022.135054

[37] Asming, M.A.A., Ibrahim, A.M. and Abir, I.M. (2022) Processing and Classification of Landsat and Sentinel Images for Oil Palm Plantation Detection. *Remote Sensing Applications: Society and Environment*, **26**, Article ID: 100747. https://doi.org/10.1016/j.rsase.2022.100747

[38] Miranda, J.d.R., Alves, M.d.C., Pozza, E.A. and Santos Neto, H. (2020) Detection of Coffee Berry Necrosis by Digital Image Processing of Landsat 8 Oli Satellite Imagery. *International Journal of Applied Earth Observation and Geoinformation*, **85**, Article ID: 101983. https://doi.org/10.1016/j.jag.2019.101983

[39] Page, B.P., Olmanson, L.G. and Mishra, D.R. (2019) A Harmonized Image Processing Workflow Using Sentinel-2/MSI and Landsat-8/OLI for Mapping Water Clarity in Optically Variable Lake Systems. *Remote Sensing of Environment*, **231**, Article ID: 111284. https://doi.org/10.1016/j.rse.2019.111284

[40] Shen, F., Li, J. and Chen, Z. (2025) Comment on "Remote Sensing Estimation of Dissolved Organic Carbon Concentrations in Chinese Lakes Based on Landsat Images" by Zhilong Zhao, Kun Shi and Yunlin Zhang. *Journal of Hydrology*, **662**, Article ID: 133990. https://doi.org/10.1016/j.jhydrol.2025.133990

[41] Yan, L. and Roy, D.P. (2025) Using Landsat 8 and 9 Operational Land Imager (OLI) Data to Characterize Geometric Distortion and Improve Geometric Correction of Landsat Multispectral Scanner (MSS) Imagery. *Remote Sensing of Environment*, **321**, Article ID: 114679. https://doi.org/10.1016/j.rse.2025.114679

[42] Aires, U.R.V., Martins, V.S., Ferreira, L.B., Huang, Y., Heintzman, L. and Ouyang, Y. (2025) Impact of Sampling Techniques on Crop Type Mapping Using Multi-Temporal Composites from Harmonized Landsat-Sentinel Images. *Computers and Electronics in Agriculture*, **237**, Article ID: 110676. https://doi.org/10.1016/j.compag.2025.110676

[43] Costanza, R. (2020) Valuing Natural Capital and Ecosystem Services toward the Goals of Efficiency, Fairness, and Sustainability. *Ecosystem Services*, **43**, Article ID: 101096. https://doi.org/10.1016/j.ecoser.2020.101096

[44] Chen, H., Costanza, R., Kubiszewski, I., Sloggy, M.R., Wu, L. and Zhang, T. (2024) Integrating Online Deliberation into Ecosystem Service Valuation. *Journal of Environmental Management*, **351**, Article ID: 119796. https://doi.org/10.1016/j.jenvman.2023.119796

[45] Abd-Elmaboud, M.E., Saqr, A.M., El-Rawy, M., Al-Arifi, N. and Ezzeldin, R. (2024) Evaluation of Groundwater Potential Using Ann-Based Mountain Gazelle Optimization: A Framework to Achieve Sdgs in East El Oweinat, Egypt. *Journal of Hydrology: Regional Studies*, **52**, Article ID: 101703. https://doi.org/10.1016/j.ejrh.2024.101703

[46] Alarifi, S.S., Abdelrahman, K. and Hazaea, B.Y. (2022) Depicting of Groundwater Potential in Hard Rocks of Southwestern Saudi Arabia Using the Vertical Electrical Sounding Approach. *Journal of King Saud University—Science*, **34**, Article ID: 102221. https://doi.org/10.1016/j.jksus.2022.102221

[47] Arefin, R. (2020) Groundwater Potential Zone Identification at Plio-Pleistocene Elevated Tract, Bangladesh: AHP-GIS and Remote Sensing Approach. *Groundwater for Sustainable Development*, **10**, Article ID: 100340. https://doi.org/10.1016/j.gsd.2020.100340

[48] Bhadran, A., Girishbai, D., Jesiya, N.P., Gopinath, G., Krishnan, R.G. and Vijesh, V.K. (2022) A GIS Based Fuzzy-AHP for Delineating Groundwater Potential Zones in Tropical River Basin, Southern Part of India. *Geosystems and Geoenvironment*, **1**, Article ID: 100093. https://doi.org/10.1016/j.geogeo.2022.100093

[49] Boum-Nkot, S.N., Nlend, B., Komba, D., Ndondo, G.R.N., Bello, M., Fongoh, E.J., *et al.* (2023) Hydrochemistry and Assessment of Heavy Metals Groundwater Contamination in an Industrialized City of Sub-Saharan Africa (Douala, Cameroon). Implication on Human Health. *HydroResearch*, **6**, 52-64. https://doi.org/10.1016/j.hydres.2023.01.003

[50] Choudhury, T.R., Moniruzzaman, M., Anonna, T.A., Asad, H.A., Samanta, P. and Islam, F. (2025) Evaluation of Heavy Metal Contamination in Soil, Water, and Fish in an Industrial Zone in Bangladesh: Ecological and Potential Health Risk. *Regional*

Studies in Marine Science, **86**, Article ID: 104162. https://doi.org/10.1016/j.rsma.2025.104162

[51] Czauner, B., Simon, S. and Mádl-Szőnyi, J. (2024) How to Consider Groundwater Flow Systems in the Earth's Critical Zone?—Demonstration in the Central Pannonian Basin, Hungary. *Journal of Hydrology: Regional Studies*, **53**, Article ID: 101833. https://doi.org/10.1016/j.ejrh.2024.101833

[52] Dhinsa, D., Tamiru, F. and Tadesa, B. (2022) Groundwater Potential Zonation Using VES and GIS Techniques: A Case Study of Weserbi Guto Catchment in Sululta, Oromia, Ethiopia. *Heliyon*, **8**, e10245. https://doi.org/10.1016/j.heliyon.2022.e10245

[53] Ejaz, N., Khan, A.H., Saleem, M.W., Elfeki, A.M., Rahman, K.U., Hussain, S., *et al.* (2024) Multi-Criteria Decision-Making Techniques for Groundwater Potentiality Mapping in Arid Regions: A Case Study of Wadi Yiba, Kingdom of Saudi Arabia. *Groundwater for Sustainable Development*, **26**, Article ID: 101223. https://doi.org/10.1016/j.gsd.2024.101223

[54] El-Sayed, H.M. and Elgendy, A.R. (2024) Geospatial and Geophysical Insights for Groundwater Potential Zones Mapping and Aquifer Evaluation at Wadi Abu Marzouk in El-Nagila, Egypt. *Egyptian Journal of Aquatic Research*, **50**, 23-35. https://doi.org/10.1016/j.ejar.2023.12.008

[55] Falowo, O.O. and Ojo, O. (2023) Multi-criteria Groundwater Potential Zonation Using GIS-Based Fuzzified AHP: Case Study of Ondo Metropolis Southwestern Nigeria. *Solid Earth Sciences*, **8**, 319-344. https://doi.org/10.1016/j.sesci.2023.11.002

[56] Fildes, S.G., Bruce, D., Clark, I.F., Raimondo, T., Keane, R. and Batelaan, O. (2022) Integrating Spatially Explicit Sensitivity and Uncertainty Analysis in a Multi-Criteria Decision Analysis-Based Groundwater Potential Zone Model. *Journal of Hydrology*, **610**, Article ID: 127837. https://doi.org/10.1016/j.jhydrol.2022.127837

[57] Fotsing Metegam, I.F. (2025) Monte Carlo and Fuzzy AHP with GIS for Ranking Hybrid Solar-Wind Sites for Electricity and Hydrogen Production in Cameroon. *International Journal of Hydrogen Energy*, **106**, 741-766. https://doi.org/10.1016/j.ijhydene.2025.01.418

[58] Gaur, S., Chahar, B.R. and Graillot, D. (2011) Combined Use of Groundwater Modeling and Potential Zone Analysis for Management of Groundwater. *International Journal of Applied Earth Observation and Geoinformation*, **13**, 127-139. https://doi.org/10.1016/j.jag.2010.09.001

[59] Martínez de Icaya-Gómez, E., Martínez-Izquierdo, E., Hernández-Viñas, M. and Naranjo-Hernández, J.E. (2025) Reduced Dimensionality Space of Features Using Spectral Indices for Detecting Changes in Multitemporal Landsat-8 Images. *Ecological Informatics*, **87**, Article ID: 103090. https://doi.org/10.1016/j.ecoinf.2025.103090

[60] Gidafie, D., Nedaw, D. and Azagegn, T. (2024) Integrated Remote Sensing and Geographic Information System Overlay Analysis for Groundwater Potential Evaluation Using AHP and Fuzzy AHP: Southern Sections of the Western Afar Rift Margin and Associated Rift Floor. *Groundwater for Sustainable Development*, **26**, Article ID: 101310. https://doi.org/10.1016/j.gsd.2024.101310

[61] Li, J., Jiang, Z., Miao, H., Liang, J., Yang, Z., Zhang, Y., *et al.* (2022) Identification of Cultivated Land Change Trajectory and Analysis of Its Process Characteristics Using Time-Series Landsat Images: A Study in the Overlapping Areas of Crop and Mineral Production in Yanzhou City, China. *Science of the Total Environment*, **806**, Article ID: 150318. https://doi.org/10.1016/j.scitotenv.2021.150318

[62] Abdelmalik, K.W. (2020) Landsat 8: Utilizing Sensitive Response Bands Concept for Image Processing and Mapping of Basalts. *The Egyptian Journal of Remote Sensing*

and Space Science, **23**, 263-274. https://doi.org/10.1016/j.ejrs.2019.04.004

[63] Al-Obeidat, F., Al-Taani, A.T., Belacel, N., Feltrin, L. and Banerjee, N. (2015) A Fuzzy Decision Tree for Processing Satellite Images and Landsat Data. *Procedia Computer Science*, **52**, 1192-1197. https://doi.org/10.1016/j.procs.2015.05.157

[64] Sambandham, V.T., Kirchheim, K., Ortmeier, F. and Mukhopadhaya, S. (2024) Deep Learning-Based Harmonization and Super-Resolution of Landsat-8 and Sentinel-2 Images. *ISPRS Journal of Photogrammetry and Remote Sensing*, **212**, 274-288. https://doi.org/10.1016/j.isprsjprs.2024.04.026

[65] Lasanta, T. and Vicente-Serrano, S.M. (2012) Complex Land Cover Change Processes in Semiarid Mediterranean Regions: An Approach Using Landsat Images in Northeast Spain. *Remote Sensing of Environment*, **124**, 1-14. https://doi.org/10.1016/j.rse.2012.04.023

[66] Härkönen, S., Lehtonen, A., Eerikäinen, K., Peltoniemi, M. and Mäkelä, A. (2011) Estimating Forest Carbon Fluxes for Large Regions Based on Process-Based Modelling, NFI Data and Landsat Satellite Images. *Forest Ecology and Management*, **262**, 2364-2377. https://doi.org/10.1016/j.foreco.2011.08.035

[67] Chen, S., Wang, G., Xu, X., Ouyang, Z., Li, R., Remo, J.W., *et al.* (2025) A Mixed Training Sample-Based Spectral Unmixing Analysis for Improving Fractional Abundance Estimation of Detroit Landscape Endmembers Using Landsat Images. *Urban Forestry & Urban Greening*, **107**, Article ID: 128786. https://doi.org/10.1016/j.ufug.2025.128786

[68] Li, J., Wang, Y., Sheng, Q., Wu, Z., Wang, B., Ling, X., *et al.* (2025) Cloudruler: Rule-Based Transformer for Cloud Removal in Landsat Images. *Remote Sensing of Environment*, **328**, Article ID: 114913. https://doi.org/10.1016/j.rse.2025.114913

[69] Cormier, E.C., Devred, E., Wilson, K.L., Smukall, M.J., Fuentes, M.M.P.B. and Lotze, H.K. (2025) Analysis of Two Decades of Landsat Satellite Images Reveals Long-Term Changes in Aquatic and Terrestrial Vegetation in Bimini, the Bahamas with Coastal Development. *FACETS*, **10**, 1-18. https://doi.org/10.1139/facets-2024-0020

[70] Suneetha, C., Kumar, L.S., Sreenivas, K. and Mitran, T. (2025) Deep Learning-Driven Soil Texture Classifier Using Landsat 8 Images. *Remote Sensing Applications: Society and Environment*, **38**, Article ID: 101568. https://doi.org/10.1016/j.rsase.2025.101568

[71] Gunsola, A., Nautiyal, A. and Bhatia, S.Y. (2025) LULC Classification of Tehri Region Using Landsat 7 & 8 Satellite Images. *Procedia Computer Science*, **260**, 957-963. https://doi.org/10.1016/j.procs.2025.03.279

[72] Badamfirooz, J., Mousazadeh, R. and Sarkheil, H. (2021) A Proposed Framework for Economic Valuation and Assessment of Damages Cost to National Wetlands Ecosystem Services Using the Benefit-Transfer Approach. *Environmental Challenges*, **5**, Article ID: 100303. https://doi.org/10.1016/j.envc.2021.100303

[73] Sobhani, P., Esmaeilzadeh, H. and Mobarghaei Dinan, N. (2025) Prioritization and Valuation of Ecosystem Services in Protected Areas. *Journal for Nature Conservation*, **84**, Article ID: 126804. https://doi.org/10.1016/j.jnc.2024.126804

[74] Bezerra, L.A.V., Garcez, D.S., Campos da Silva, M., Gurgel-Lourenço, R.C., Pinto, L.M., Valentim, G.A., *et al.* (2025) Brvaluation: A Systematic Comparison of Ecosystem Services across Brazilian Biomes and Ecosystems. *Environmental Development*, **56**, Article ID: 101279. https://doi.org/10.1016/j.envdev.2025.101279

[75] Dashtbozorgi, F., Hedayatiaghmashhadi, A., Dashtbozorgi, A., Ruiz-Agudelo, C.A., Fürst, C., Cirella, G.T., *et al.* (2023) Ecosystem Services Valuation Using Invest Modeling: Case from Southern Iranian Mangrove Forests. *Regional Studies in Marine Science*, **60**, Article ID: 102813. https://doi.org/10.1016/j.rsma.2023.102813

[76] Garshasbi, F., Ashournejad, Q. and Ghalenoei, N. (2025) A Comparative Assessment of Remote Sensing Based Land Cover Products for Economic Valuation of Ecosystem Services of Hyrcanian Forests. *Advances in Space Research*, **75**, 4552-4574. https://doi.org/10.1016/j.asr.2024.12.064

[77] Mono, J.A., Bouba, A., Ngoh, J.D., Amougou, O.U.I.O., Nyam, F.M.E.A. and Mbarga, T.N. (2024) Lineament Mapping in Batie Area (West-Cameroon) Using Landsat-9 Operational Land Imager/thermal Infrared Sensor and Shuttle Radar Topography Mission Data: Hydrogeological Implication. *Revue Internationale de Géomatique*, **33**, 135-154. https://doi.org/10.32604/rig.2024.049966

[78] Himes-Cornell, A., Pendleton, L. and Atiyah, P. (2018) Valuing Ecosystem Services from Blue Forests: A Systematic Review of the Valuation of Salt Marshes, Sea Grass Beds and Mangrove Forests. *Ecosystem Services*, **30**, 36-48. https://doi.org/10.1016/j.ecoser.2018.01.006

[79] Naime, J., Mora, F., Sánchez-Martínez, M., Arreola, F. and Balvanera, P. (2020) Economic Valuation of Ecosystem Services from Secondary Tropical Forests: Trade-Offs and Implications for Policy Making. *Forest Ecology and Management*, **473**, Article ID: 118294. https://doi.org/10.1016/j.foreco.2020.118294

[80] Duan, C., *et al.* (2025) Monitoring Abandoned Cropland in the Hilly and Gully Regions of the Loess Plateau Using Landsat Time Series Images. *Journal of Integrative Agriculture*. https://doi.org/10.1016/j.jia.2025.04.021

[81] Altuwaijri, H.A., Kafy, A.A. and Rahaman, Z.A. (2025) Multi-temporal Remote Sensing and Geospatial Analysis for Urban Ecosystem Service Dynamics: A Three-Decade Assessment of Land Surface Transformation in Jeddah, Saudi Arabia. *Physics and Chemistry of the Earth, Parts A/B/C*, **139**, Article ID: 103892. https://doi.org/10.1016/j.pce.2025.103892